

# Supplementary Material

## Limited impact of climate forcing products on future glacier evolution in Scandinavia and Iceland

Loris COMPAGNO<sup>1,2</sup>, Harry ZEKOLLARI,<sup>3,4,1,2</sup> Matthias HUSS<sup>1,2,5</sup>, Daniel FARINOTTI<sup>1,2</sup>

<sup>1</sup>Laboratory of Hydraulics, Hydrology and Glaciology (VAW), ETH Zurich, Zurich, Switzerland.

<sup>2</sup>Swiss Federal Institute for Forest, Snow and Landscape Research (WSL), Birmensdorf, Switzerland.

<sup>3</sup>Department of Geoscience and Remote Sensing, Delft University of Technology, Netherlands

<sup>4</sup>Laboratoire de Glaciologie, Université libre de Bruxelles, Belgium

<sup>5</sup>Department of Geosciences, University of Fribourg, Fribourg, Switzerland

Correspondence: Loris Compagno <compagno@vaw.baug.ethz.ch>

The Supplementary Material consist of 1 addendum concerning the 'Methods', and includes 8 figures and 2 tables.

# 1 S1 Glacier geometry initialisation method

2 The GloGEMflow model is initialised by reproducing the glacier geometry (volume and length) at  
 3 the inventory-year. For doing this, a glacier steady state is first generated before the inventory-  
 4 year. This is realized by forcing both the SMB and ice flow model with a constant climate over the  
 5 period  $t_{s,1} - t_{s,2}$  (Fig. S1). The start-year ( $t_{s,1}$ ) and end-year ( $t_{s,2}$ ) are defined by using an iterative  
 6 method that takes both glacier response time and climate into account:  $t_{s,2}$  is computed for each  
 7 glacier individually, and is defined as

$$t_{s,2} = t_i - 0.5 \Delta t_r, \quad (1)$$

8 where  $t_i$  is the glacier inventory-year (see Table S1) and  $\Delta t_r$  is the glacier response time calculated  
 9 using the approach of Jóhannesson and others (1989):

$$\Delta t_r = |\overline{H} / \overline{b_{\text{lowest}}}|. \quad (2)$$

10 Here,  $\overline{H}$  is the mean glacier thickness and  $\overline{b_{\text{lowest}}}$  the SMB at the lowest glacier point at the  
 11 inventory-year (averaged over  $\pm 2$  years, to avoid the effect of seasonality). The empirical factor  
 12 0.5 in Equation 1 ensures that the produced steady state geometry at  $t_{s,2}$  preserves an influence on  
 13 the glacier length at the inventory-year. This is crucial for the initialisation procedure, as no useful  
 14 information would be preserved if the initial and transient glacier geometries would be separated  
 15 by a long time period (Zekollari and others, 2019; Eis and others, 2019). Typical values for  $\Delta t_r$   
 16 are between 10 and 44 years.  $t_{s,1}$  is chosen so that the time span ( $\Delta t_s = t_{s,1} - t_{s,2}$ ) covers the time  
 17 period during which the integrated glacier SMB is as close as possible to zero. If  $b_s(i)$  is the glacier  
 18 SMB for year  $i$ , this procedure can be expressed as:

$$B_n = \sum_{i=1}^n b_s(t_{s,1} + i), \quad (3)$$

$$B = \{B_n \mid n = [10, t_{\text{max}}]\}, \quad (4)$$

$$B_{\text{min}} : \min(B), \quad (5)$$

$$\Delta t_s = n \text{ for } B = B_{\text{min}}, \quad (6)$$

$$t_{s,1} = t_{s,2} - \Delta t_s. \quad (7)$$

19 In the equations above,  $B_n$  is the cumulative SMB for a time period of candidate length  $n$ , where  
 20  $n$  has an empiric minimum of 10 years and a maximum of  $t_{\text{max}}$  years.  $t_{\text{max}}$  is computed as

$$t_{\text{max}} = t_{s,2} - t_0, \quad (8)$$

21 where  $t_0$  is 1950 for E-OBS and 1979 for ERA.  $B$  is the set of all possible  $B_n$ 's, and  $B_{\text{min}}$  is the  
 22 minimal value of  $B$ . Since no information about the glacier geometry exist initially, the glacier area

required to compute  $b_s$  is computed using the following iterative method. In the first iteration, the area of the inventory-year is used, and a steady state glacier is produced. At every subsequent iteration, the area is updated with the result of the steady state of the previous iteration (Fig.S1). The procedure is repeated until the difference between the area of two subsequent iterations is less than 1%. It is important to note that the obtained steady-state geometry is only used for model initialization, and that the procedure does not imply, for example, that the glacier was actually in balance during the period delimited by  $t_{s,1}$  and  $t_{s,2}$ .

After the initial glacier geometry has been determined, the glacier evolution until the inventory-year is simulated by forcing the model with the past climate dataset (ERA-I, ERA-5 or E-OBS). By iteratively modifying the deformation-sliding factor and the steady state SMB, the modelled glacier volume and length are matched with the observations at the inventory-year (Fig. S1). The deformation-sliding factor mainly determines the volume at the inventory-year, whilst the SMB offset is the main driver for the glacier length at steady state, and thus also at the inventory date (Zekollari and others, 2019). The mean deformation-sliding factor of Scandinavia (Iceland) is of  $1.2 \times 10^{-16} \text{ Pa}^{-1} \text{ yr}^{-1}$  ( $3.2 \times 10^{-16} \text{ Pa}^{-1} \text{ yr}^{-1}$ ), with a standard deviation.  $1.2 \times 10^{-16} \text{ Pa}^{-1} \text{ yr}^{-1}$  ( $3.6 \times 10^{-16} \text{ Pa}^{-1} \text{ yr}^{-1}$ ). An optimization procedure is used in between the iterations. The information of the previously iteration are taken into account, so that the modelled volume and length at the inventory-year converge efficiently to the values at inventory-year (for more details see Zekollari and others, 2019).

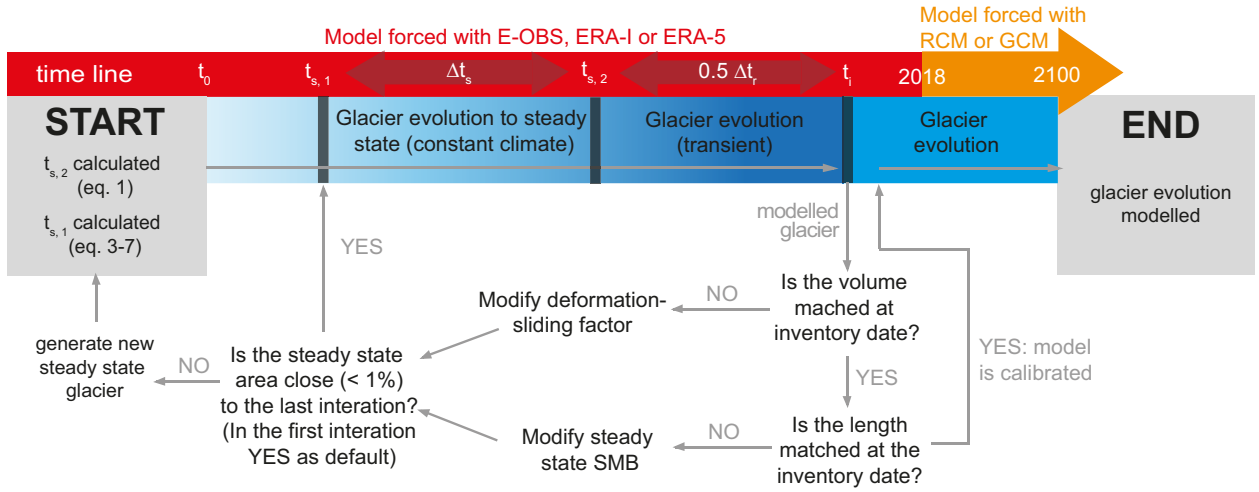


Figure S1: Procedure used to initialise the glacier geometry at the inventory-year.  $t_{s,1}$  and  $t_{s,2}$  are the start- and end-year of the constant climate forcing period, respectively.  $t_i$  is the inventory-year, and  $\Delta t_r$  is the response time. All variables are glacier specific.

Initially, GloGEMflow was successful in modelling the future evolution of about 95% of all glaciers. For the remaining 5% numerical problems arose because of steep steps in the bedrock and very narrow widths at the glacier terminus. These problems were solved by smoothing the steep bedrock steps with a running mean (window length = 3% of the glacier length at the inventory-year) and by applying a threshold for the minimum glacier width in the lowermost 30% of the glacier. This threshold was set to 20% of the mean glacier width.

## 48 S2 Supplementary Figures

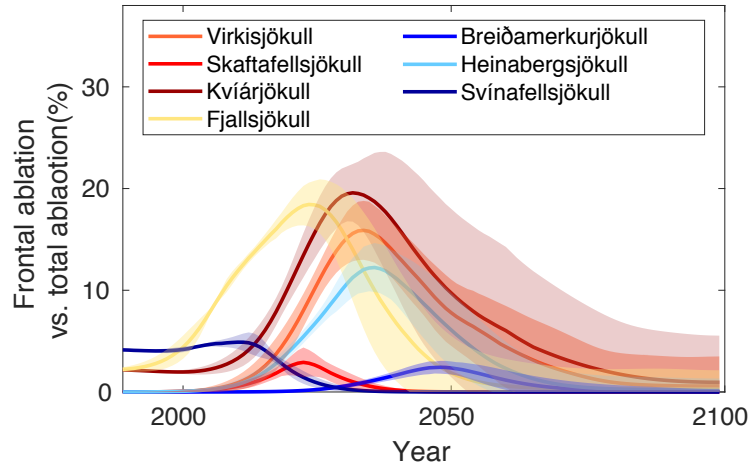


Figure S2: Frontal ablation rate for seven Icelandic glaciers compared to total ablation. Each line represent one glacier. The transparent band correspond to one standard deviation of all 51 RCMs.

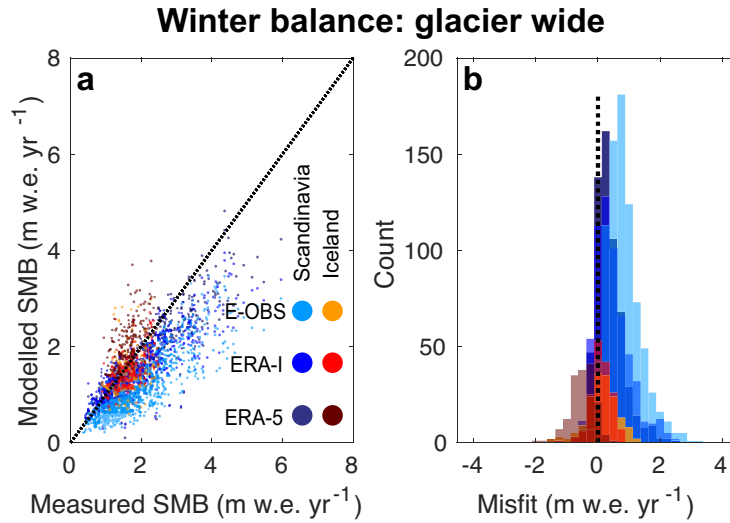


Figure S3: Evaluation of modelled winter SMB versus glacier-wide WGMS observations. Colours tending to red represent Icelandic glaciers, colours tending to blue represents Scandinavian glaciers. The colour's tone discerns between individual climate datasets.

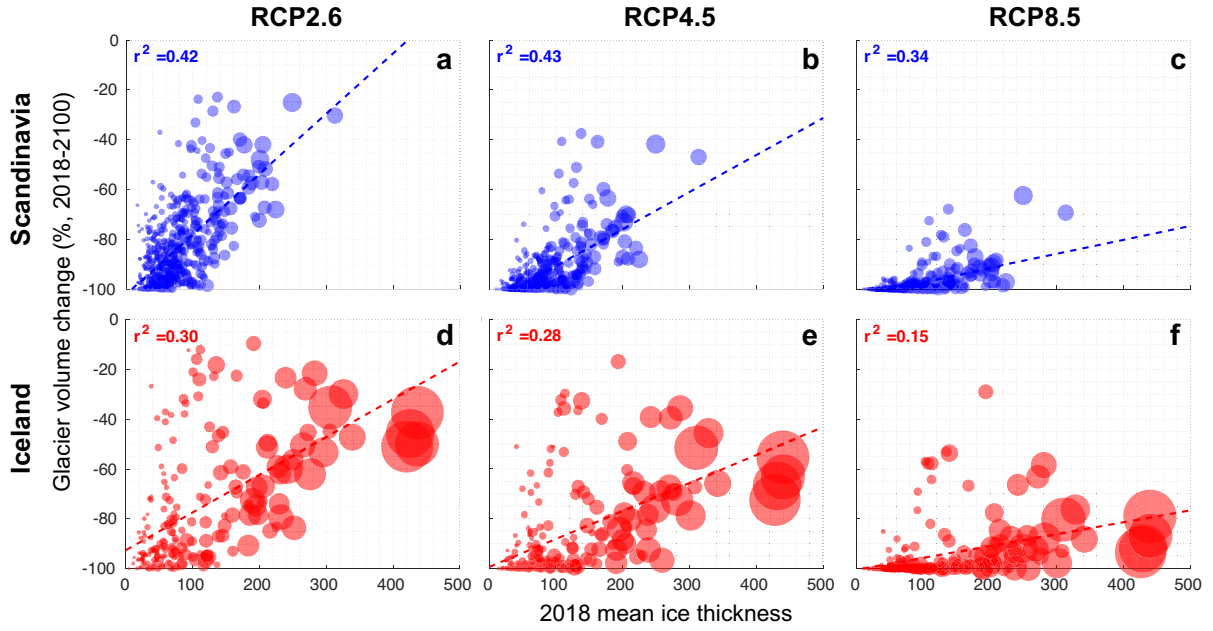


Figure S4: Volume change as a function mean ice thickness for Scandinavia (a–c) and Iceland (d–f). The size of the circles indicates the glacier volume. The dashed lines are a linear fit through the cloud of circles. The fit’s coefficient of determination is given by  $r^2$ .

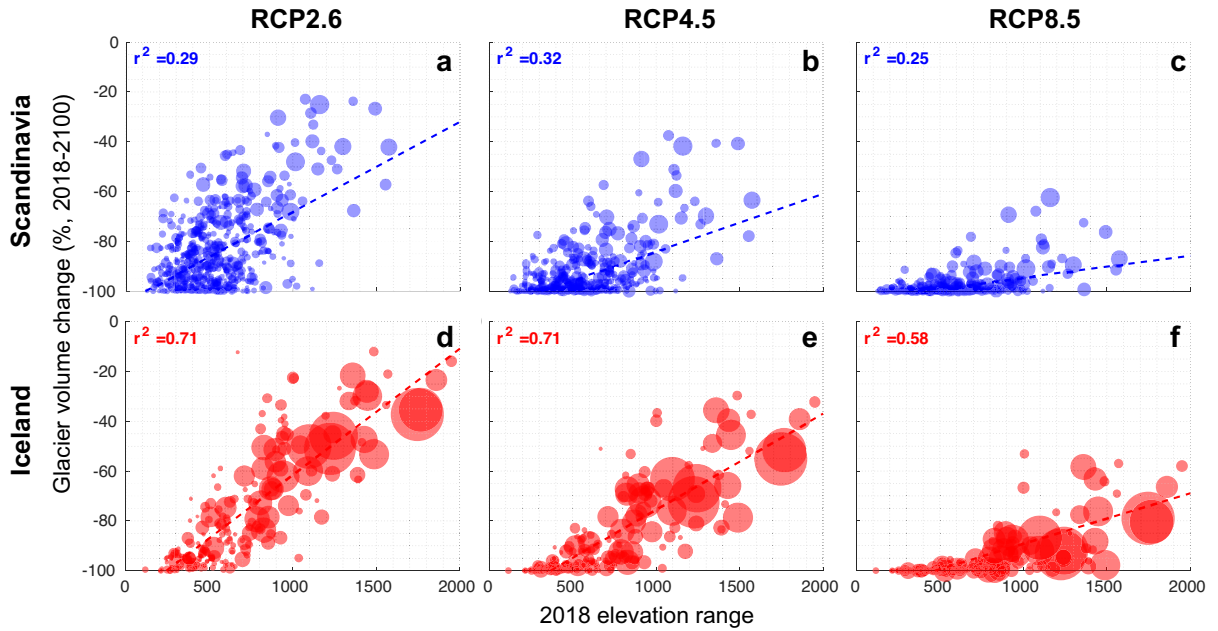


Figure S5: Same as Figure S3 but for elevation range.

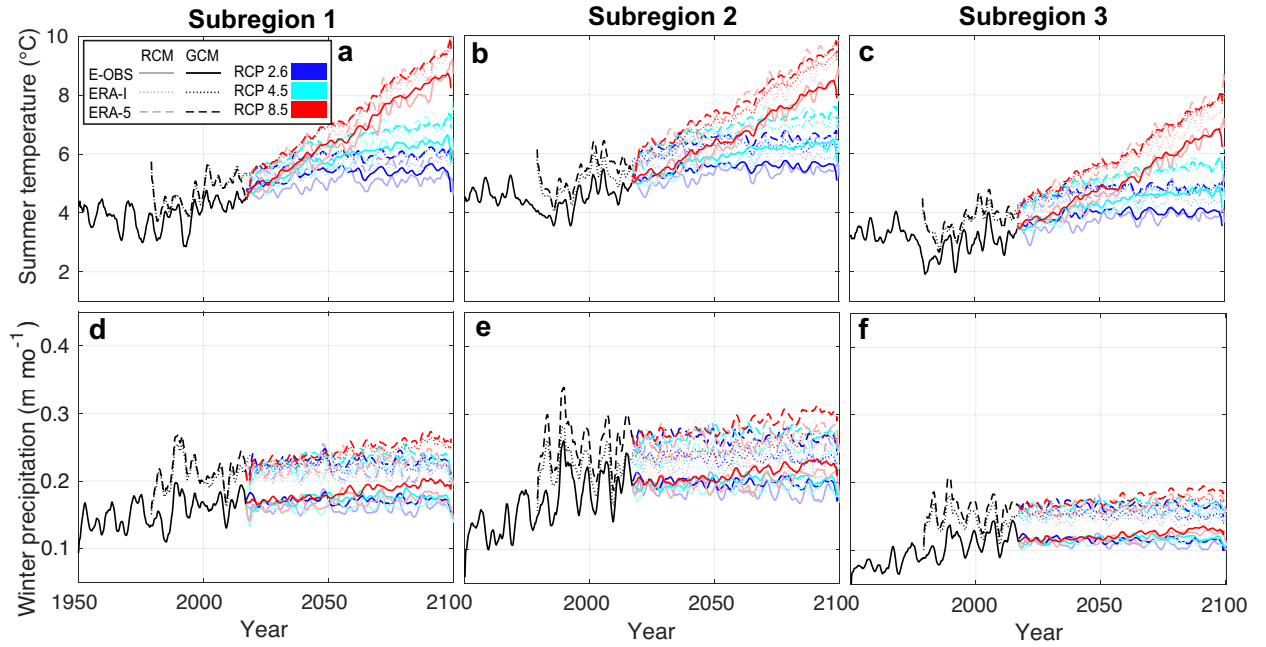


Figure S6: Average summer (1. May – 30. September) temperature (**a–c**) and winter (1. October–30. April) precipitation (**d–f**) for Scandinavian glaciers. Subregions 1(**a** & **d**), 2 (**b** & **e**) and 3 (**c** & **f**) are discerned. The provided values correspond to the average value of the climate re-analysis grid cells, weighted with the number of glaciers larger than 1 km<sup>2</sup> within each grid cell. The data are smoothed with a 24-month running mean. The line type (solid, dotted, dashed) shows the past climate dataset (E-OBS, ERA-I, ERA-5), the colour's tone (light or dark) displays the future climate projections (average of all RCM and GCM members), and the colours show the RCPs (2.6, 4.5 and 8.5). The change in variability between past and future is the result of averaging various RCM and GCM members.

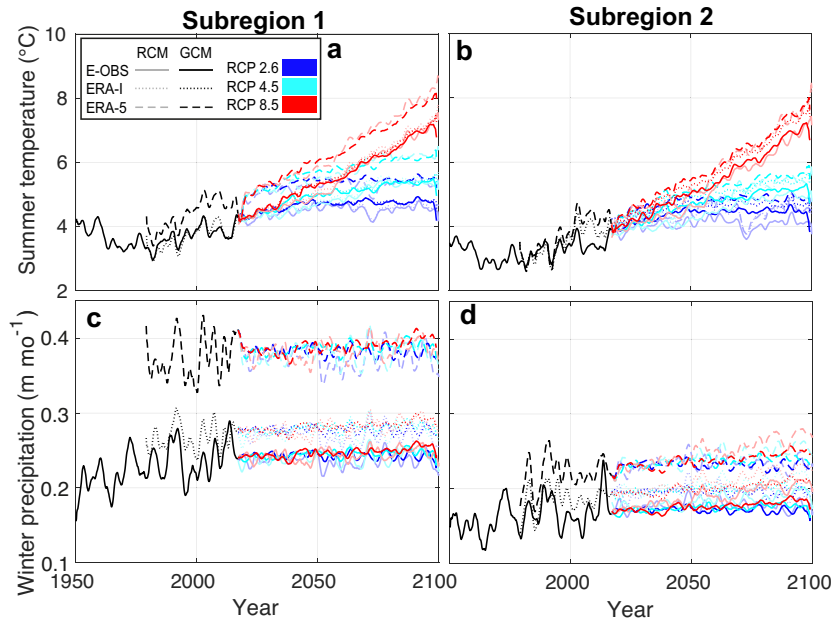


Figure S7: Same as Figure S5 but for Iceland.

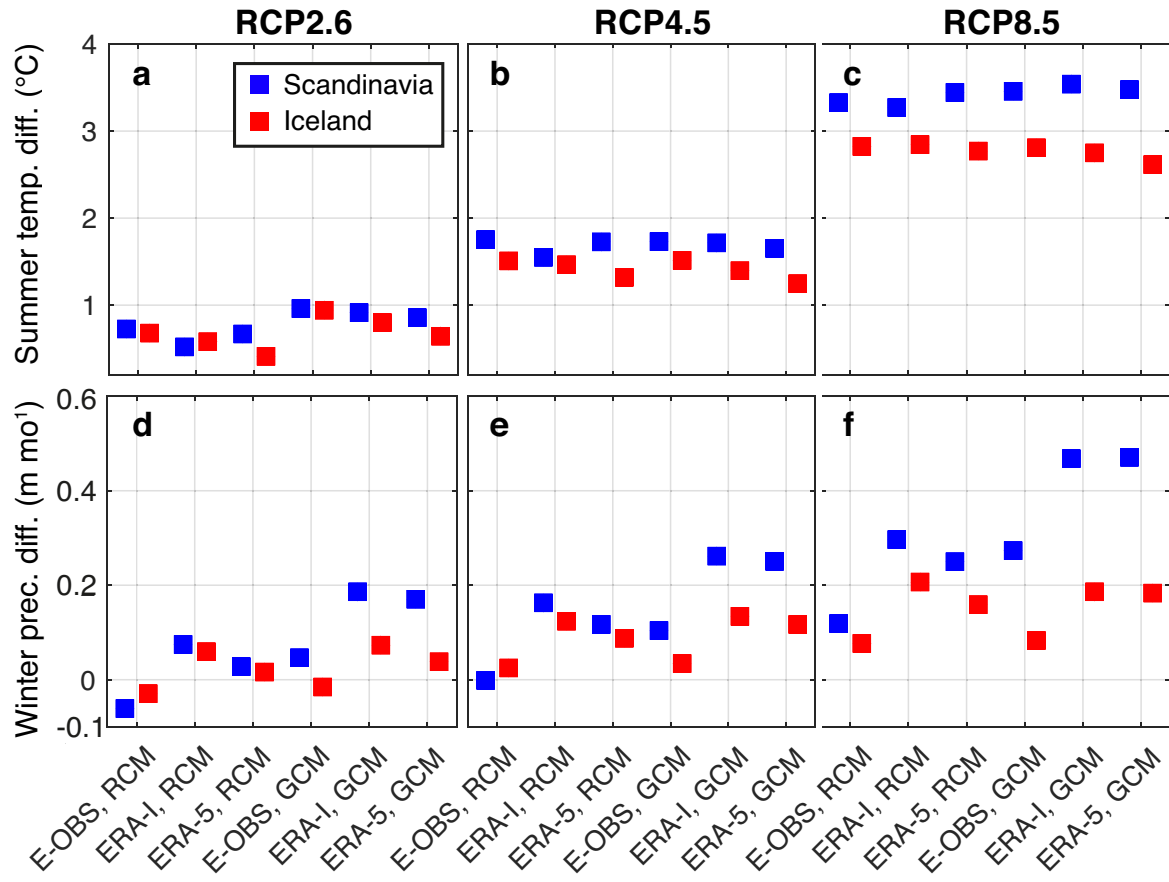


Figure S8: Mean summer temperature (a–c) and winter precipitation (d–f) difference between the calibration period 2003-2014 and 2018-2100. The x-axis shows all possible combinations of climate datasets. RCP2.6, 4.5 and 8.5 are shown separately.

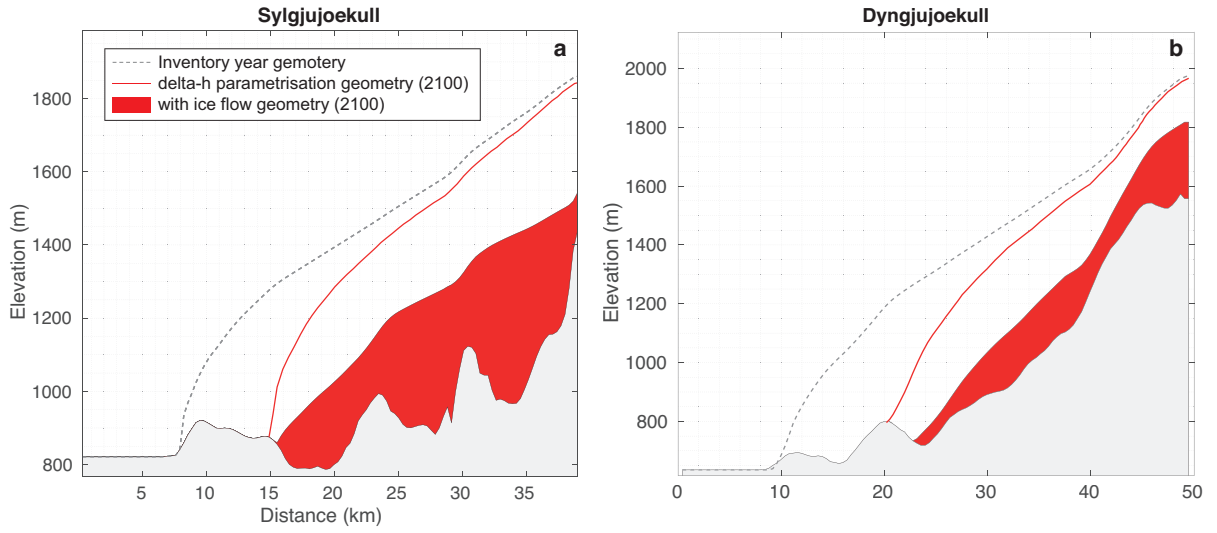


Figure S9: Cross section of (a) Sylgjujoekull and (b) Dyngjujoekull, Iceland (outlet glaciers of the Vatnaejoekull). The red area corresponds to the 2100 modelled geometry using GloGEMflow (ERA-5, RCM with RCP8.5). The red line shows the 2100 modelled geometry using the  $\Delta h$  parametrization (Huss and others, 2010; Huss and Hock, 2015). The grey dashed line shows the glacier geometry at inventory-year.



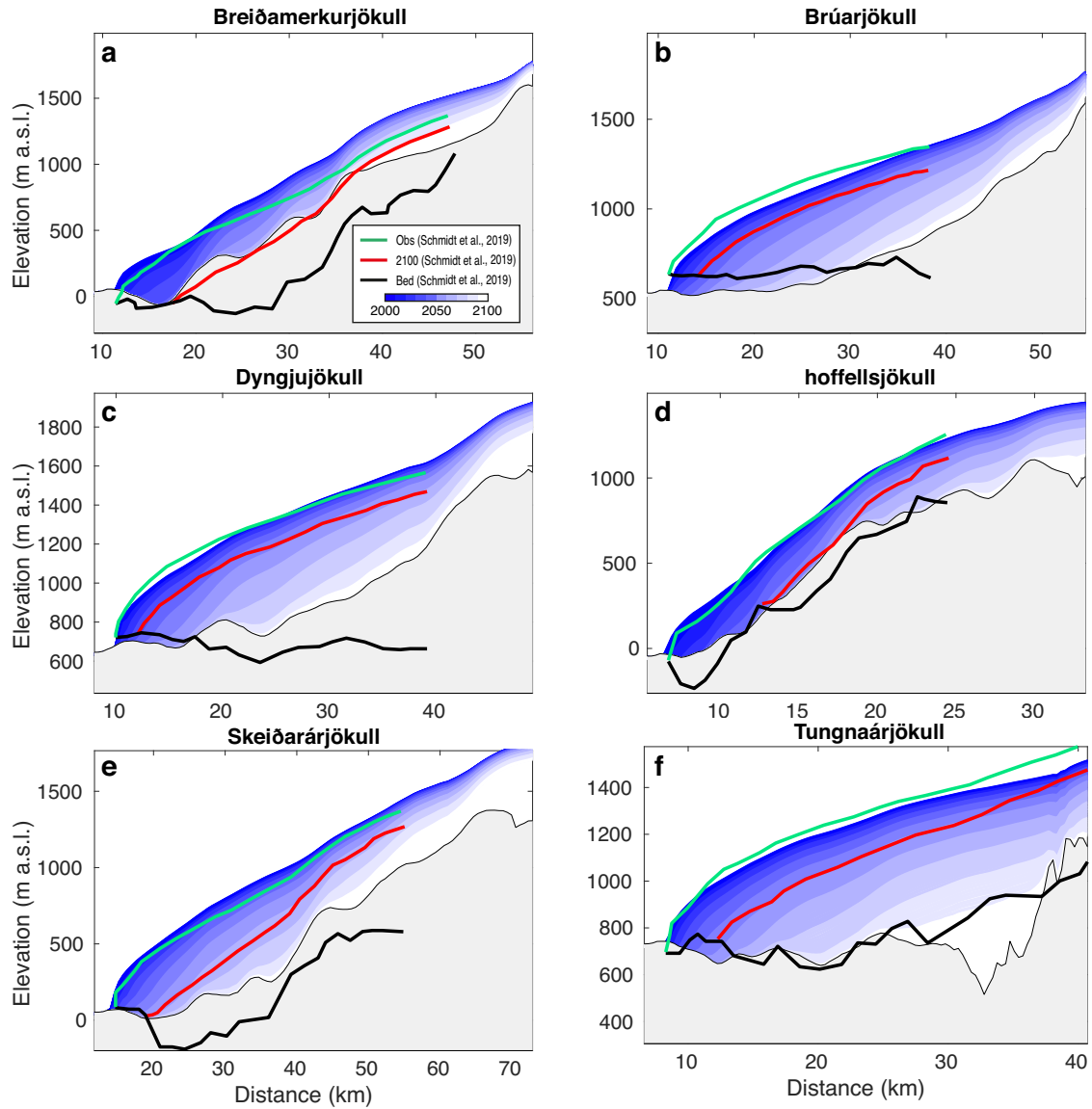


Figure S10: Future evolution (2000-2100) for six outlets of Vatnajökull ice cap under RCP 8.5. Surface and bedrock topography, as well as computed glacier surface in 2100 according to Schmidt and others (2020) are shown for comparison. Horizontal alignment between the two studies is achieved by matching the position of the present-day glacier snout.

49 **S3 Supplementary Tables**

Table S1: Overview of RGI 6.0 inventory years for Scandinavian and Icelandic glaciers. The percentages refer to the fraction of glaciers covered by a given year.

| Year | Scandinavia | Iceland |
|------|-------------|---------|
| 1999 | 19.5 %      | 10.6 %  |
| 2000 | 0 %         | 75.5 %  |
| 2001 | 23.9 %      | 0 %     |
| 2002 | 9.5 %       | 14.1 %  |
| 2003 | 14.0 %      | 10.2 %  |
| 2004 | 0 %         | 2.3 %   |
| 2005 | 0 %         | 0 %     |
| 2006 | 33.2 %      | 0 %     |

Table S2: Percentage of glaciers for which in the glacier-specific calibration the parameter sets were concluded at calibration step 1 (precipitation), 2 (DDF) or 3 (temperature), see Fig. 3 of main text.

| Past climate dataset<br>step | Scandinavia |      |     | Iceland |      |      |
|------------------------------|-------------|------|-----|---------|------|------|
|                              | 1           | 2    | 3   | 1       | 2    | 3    |
| E-OBS                        | 51 %        | 45 % | 4 % | 17 %    | 58 % | 25 % |
| ERA-I                        | 57 %        | 40 % | 3 % | 20 %    | 52 % | 28 % |
| ERA-5                        | 75 %        | 24 % | 1 % | 4 %     | 57 % | 39 % |

## Supplementary References

- Eis J, Maussion F and Marzeion B (2019) Initialization of a global glacier model based on present-day glacier geometry and past climate information: an ensemble approach. *The Cryosphere*, **13**(12), 3317–3335 (doi: 10.5194/tc-13-3317-2019)
- Huss M and Hock R (2015) A new model for global glacier change and sea-level rise. *Frontiers in Earth Science*, **3** (doi: 10.3389/feart.2015.00054)
- Huss M, Jouvett G, Farinotti D and Bauder A (2010) Future high-mountain hydrology: A new parameterization of glacier retreat. *Hydrology and Earth System Sciences*, **14**(5), 815–829 (doi: 10.5194/hess-14-815-2010)
- Jóhannesson T, Raymond C and Waddington E (1989) A simple method for determining the response time of glaciers (doi: 10.1007/978-94-015-7823-3\_22)
- Schmidt LS, Aalgeirsdóttir G, Plsson F, Langen PL, Gumundsson S and Björnsson H (2020) Dynamic simulations of Vatnajökull ice cap from 1980 to 2300. *Journal of Glaciology*, **66**(255), 97–112 (doi: 10.1017/jog.2019.90)
- Zekollari H, Huss M and Farinotti D (2019) Modelling the future evolution of glaciers in the European Alps under the EURO-CORDEX RCM ensemble. *The Cryosphere*, **13**(4), 1125–1146 (doi: 10.5194/tc-13-1125-2019)